3. *PAPER II*: KINETIC ANALYSES OF THE MAGNESIUM CHELATASE PROVIDE INSIGHTS INTO THE MECHANISM, STRUCTURE, AND FORMATION OF THE CCOMPLEX

3.1 Synopsis

- Kinetically characterized magnesium chelatase from *Rba. capsulatus* and proposed a reaction mechanism
- Determined the K_m of *Rba. capsulatus* magnesium chelatase substrates; ATP, magnesium, and proto
- BchD behaved as the enzyme, while BchI and BchH were substrates
- BchI had a 1:1 interaction with BchD, while BchH:BchD or BchH:BchI▪BchD was at least 2:1
- Additional catalysis of magnesium chelatase involving removal of Mg-proto from BchH and binding with fresh proto substrate was the slow step of the reaction mechanism
- ATPase activity was stimulated by addition of BchH to the BchI▪BchD complex and continued after magnesium chelatase activity ceased suggesting an ATP-dependent structural reorganization of magnesium chelatase subunits; BchH and BchI▪BchD in additional catalytic cycle

3.2 Journal article

Paper II

THE JOURNAL OF BIOLOGICAL CHEMISTRY VOL. 283, NO. 46, pp. 31294–31302, November 14, 2008

Kinetic Analyses of the Magnesium Chelatase Provide Insights into the Mechanism, Structure, and Formation of the Complex*[S]◆

Received for publication, July 29, 2008, and in revised form, September 9, 2008 Published, JBC Papers in Press, September 12, 2008, DOI 10.1074/jbc.M805792200

Artur Sawicki and Robert D. Willows[1]

From the Department of Chemistry and Biomolecular Sciences, Macquarie University, Sydney, New South Wales 2109, Australia

The metabolic pathway known as (bacterio)chlorophyll biosynthesis is initiated by magnesium chelatase (BchI, BchD, BchH). This first step involves insertion of magnesium into protoporphyrin IX (proto), a process requiring ATP hydrolysis. Structural information shows that the BchI and BchD subunits form a double hexameric enzyme complex, whereas BchH binds proto and can be purified as BchH-proto. We utilized the *Rhodobacter capsulatus* magnesium chelatase subunits using continuous magnesium chelatase assays and treated the BchD subunit as the enzyme with both BchI and BchH-proto as substrates. Michaelis-Menten kinetics was observed with the BchI subunit, whereas the BchH subunit exhibited sigmoidal kinetics (Hill coefficient of 1.85). The BchI·BchD complex had intrinsic ATPase activity, and addition of BchH greatly increased ATPase activity. This was concentration-dependent and gave sigmoidal kinetics, indicating there is more than one binding site for the BchH subunit on the BchI·BchD complex. ATPase activity was ~40-fold higher than magnesium chelatase activity and continued despite cessation of magnesium chelation, implying one or more secondary roles for ATP hydrolysis and possibly an as yet unknown switch required to terminate ATPase activity. One of the secondary roles for BchH-stimulated ATP hydrolysis by a BchI·BchD complex is priming of BchH to facilitate correct binding of proto to BchH in a form capable of participating in magnesium chelation. This porphyrin binding is the rate-limiting step in catalysis. These data suggest that ATP hydrolysis by the BchI·BchD complex causes a series of conformational changes in BchH to effect substrate binding, magnesium chelation, and product release.

Magnesium chelatase (EC 6.6.1.1) is an AAA^+ protein (1, 2) composed of three subunits called BchI/ChlI, BchD/ChlD, and BchH/ChlH (40, 70, and 140 kDa, respectively) and is involved in the first step of (bacterio)chlorophyll biosynthesis (3). For optimal activity, the plant/algal systems also require a fourth protein, Gun4, which binds protoporphyrin and magnesium-protoporphyrin (4–6); however, no Gun4 homolog has been identified in photosynthetic bacteria. It has been recently suggested that BchJ, thus far identified only in organisms lacking Gun4, may act as a magnesium-porphyrin chaperone *in vivo* in bacteriochlorophyll biosynthetic systems (7, 8). Magnesium chelatase appears to exist as a complex of the three aforementioned subunits and works as an ATP-dependent molecular machine (3, 9, 10). The current reaction model of magnesium chelation into the red-colored tetrapyrrole substrate, protoporphyrin IX (proto),[2] is summarized in a recent review of chlorophyll biosynthesis (11) and has been constructed through a combination of biochemical and structural data. The model was initially built from biochemical studies using plant magnesium chelatases, pea and cucumber (12, 13); and photosynthetic bacterial magnesium chelatases, *Rhodobacter capsulatus* (14), *Rhodobacter sphaeroides* (15, 16), and *Synechocystis* (17). The enzyme from the latter three organisms was purified after heterologous expression of the subunits in *Escherichia coli*. Thus far, the most detailed magnesium chelatase and ATPase kinetic studies were performed with *Synechocystis* enzyme (17–20), whereas the majority of recent structural information is from *R. capsulatus* using crystallization and electron microscopy (EM) analysis of individual subunits (21–25).

Magnesium chelation is best understood by looking at the roles of the individual enzyme subunits of the complex. The BchI subunit from *R. capsulatus* forms a hexamer upon ATP hydrolysis, and its crystal structure is known (22, 25). Hexameric BchI particles were confirmed by EM (24), whereas a heptamer was observed with the BchI homolog from *Synechocystis* (26). Only the BchI subunit has a conserved ATPase domain (3), and ATPase activity of this subunit has been confirmed (27–29), indicating this subunit is responsible for the ATP-catalyzed insertion of magnesium into proto. Studies from *Synechocystis* have shown that ~15 cycles of ATP hydrolysis are required to insert one magnesium into deuteroporphyrin, the more water-soluble analog of proto (19).

The BchD subunit has strong homology to the BchI subunit at the N terminus known as the AAA domain (22). This subunit also appears to form hexamers observed with EM; however, this oligomerization does not require ATP (21). Biochemical data first demonstrated the likely formation of a BchI·BchD complex because the lag phase of the magnesium chelatase reaction was overcome by premixing of the BchI and BchD subunits in the presence of magnesium and ATP (17). Also the BchD subunit requires the BchI subunit in the refolding process to stay solu-

* The costs of publication of this article were defrayed in part by the payment of page charges. This article must therefore be hereby marked "*advertisement*" in accordance with 18 U.S.C. Section 1734 solely to indicate this fact.
◆ This article was selected as a Paper of the Week.
[S] The on-line version of this article (available at http://www.jbc.org) contains supplemental Figs. 1 and 2.
[1] To whom correspondence should be addressed. Tel.: 61-2-9850-8146; Fax: 61-2-9850-8313; E-mail: rwillows@rna.bio.mq.edu.au.

[2] The abbreviations used are: proto, protoporphyrin IX; EM, electron microscopy; Tricine, *N*-[2-hydroxy-1,1-bis(hydroxymethyl)ethyl]glycine; DTT, dithiothreitol; Mg-proto, magnesium-protoporphyrin IX.

ble in *R. capsulatus*, although the expected double hexameric (~660 kDa) complex was never observed (14). Instead, an ~200-kDa complex has been observed in *R. sphaeroides* using size-exclusion chromatography (15). It has been shown that the BchD subunit interacts directly with the BchI subunit (15, 28, 30–32) and that magnesium chelatase activity requires the BchI subunit in excess of BchD (14, 15, 17). These results have led to the proposal that the BchI subunit may act as a chaperone for BchD (31). The lack of ATPase activity of the BchD subunit (27–29) and the absence of the required amino acid in the ATPase domain sites on the BchD subunit (22) prompted the suggestion that it could have a role as a platform for binding the BchI subunit (21). EM reconstruction of the BchI·BchD complex has been recently modeled to a double hexamer composed of a trimer of homodimers (33). Thus far, a BchI·BchD·BchH-proto complex has not been isolated, and it has been presumed to exist transiently because only weak interactions were observed with the BchD and BchH subunits (30).

The recombinantly produced *R. capsulatus* BchH subunit sequesters proto readily. For optimal magnesium chelatase activity, both the BchH and BchI subunits appear to be required in slight excess over the BchD subunit (17) presumably to form a stable BchI·BchD complex that forms in a 1:1 molar ratio (33). Both BchI and BchH subunits behave kinetically as substrates when the BchD subunit is treated as the enzyme (3). However, the K_m of the BchH subunit is ~2–3 times that of the BchI subunit, indicative of a weaker association of BchH with BchD compared with BchI (17). The structure of the BchH subunit has also been recently investigated by EM, revealing a large conformational change upon binding of the proto substrate (23).

We sought to complete the kinetic characterization of magnesium chelatase activity from *R. capsulatus* using purified subunits and to examine these results based on the current reaction model. These experiments were based primarily upon continuous assays. Our data provide more accurate initial rates than previous results obtained from *R. capsulatus* using minute-scale stopped assays (14). The results provide kinetic profiles of the BchI, BchD, and BchH subunits and highlight some similarities to and differences from previous reports on *R. sphaeroides* and *Synechocystis* (15, 17). These new findings shed new light in terms of the currently proposed reaction model, regulation of enzyme activity, stability of the complex, and the roles of ATP hydrolysis in the reaction cycle of the complex.

EXPERIMENTAL PROCEDURES

Materials—All chemicals were from Sigma, Astral Scientific, and Ajax Finechem unless stated otherwise.

Protein Determination—The protein concentrations of BchI and His_6-tagged BchD were determined using the Bradford method (34). The His_6-tagged BchH concentration was determined using a molar extinction coefficient of $\epsilon_{280} = 118{,}600\ M^{-1}\ cm^{-1}$ and a molecular mass of 132,000 g/mol. All errors and error bars are shown as means ± S.E. unless stated otherwise.

BchH:Proto Ratio—The proto concentration bound to the BchH subunit was determined by adding an aliquot of purified BchH to an excess of 80% (v/v) acetone and 20% (v/v) 1 M ammonia (acetone/ammonia) and immediately vortexing. The solution was centrifuged at 18,000 × *g* for 5 min at room temperature, and the supernatant was used to measure the amount of proto present using a PerkinElmer Life Sciences LS 55 luminescence spectrometer and referring to a standard curve at $Ex_{400\ nm}$ and $Em_{630\ nm}$. The BchH used in the experiments had a protein:proto ratio of 1.24–3.26:1.

Porphyrin Solutions—Stock solutions of proto and Mg-proto were prepared as described previously (35).

Protein Expression and Purification—BchI and His_6-tagged BchD were purified as described (14, 36) with the modifications that a Superose 6 column was used for the final purification step of BchI, and 1% (v/v) Triton X-100 was used to wash the inclusion bodies of expressed BchD. His_6-tagged BchH was purified according to Willows and Beale (14) by Ni^{2+} affinity chromatography with a final wash step of 40 mM imidazole. BchH was then desalted into 5 mM Tricine-NaOH (pH 8.0) and concentrated (30-kDa cutoff membrane, Millipore) before further purification by anion-exchange chromatography using Source 15Q resin (GE Healthcare). A 10/100 column with a 6-ml bed volume was used at a flow rate of 3 ml/min and a linear gradient from 0 to 75% buffer (5 mM Tricine-NaOH (pH 8.0) with 1 M NaCl) over 20 column volumes with 1.5-ml fractions collected over this range. The red-colored fractions containing purified BchH eluted between ~51 and 60 ml (~0.32–0.37 M NaCl), and these samples were analyzed by SDS-PAGE before the purest fractions were pooled.

Magnesium Chelatase Assays—All assays were performed according to Axelsson *et al.* (21) with the following modifications. The final concentrations were 50 mM Tricine-NaOH (pH 8.0), 21 mM glycerol, 15 mM $MgCl_2$, 3.26 mM urea, 2 mM dithiothreitol (DTT), 1 mM ATP (assay buffer), 367 nM BchH-proto, 263 nM BchI, and 31.7 nM BchD unless stated otherwise in the figure or table legends. Approximately 0.5-μl aliquots of BchD in 6 M urea buffer (50 mM Tricine-NaOH (pH 8.0), 15 mM $MgCl_2$, and 4 mM DTT) were refolded with rapid addition of 700 μl of variable concentrations of BchI (at least 0.5:1 BchI:BchD) on ice giving 63.3 nM BchD and incubated for 2 h. Assays were started by addition of 100 μl of BchI·BchD and 100 μl of BchH. For continuous assays, fluorescence readings using a gain of 20 were taken immediately with readings every 4–9 s. and the initial rates measured. The standard curve for continuous assays involved reacting BchI·BchD·BchH-proto with 100 μM Tween 80 and different BchH-proto concentrations until a base-line rate was reached. A linear amount of BchI·BchD·BchH-Mg-proto was made corresponding to a starting BchH-proto concentration of between 3.8 and 120 nM. The assay with 120 nM was stopped with acetone/ammonia and separated by high pressure liquid chromatography (5–67% acetonitrile over 15 min) using a previous method (35). The conversion to BchI·BchD·BchH-Mg-proto was estimated at 87% using various mixtures of proto/Mg-proto concentrations as standards. This was taken into account when the final Mg-proto standard curve was constructed over the various porphyrin concentrations. Stopped assays involved taking a 150-μl sample and adding to 150 or 200 μl of acetone/ammonia. After centrifugation at 18,000 × *g* for 5 min at room temperature, 250 μl of the supernatant was used for spectrofluorometry ($Ex_{418\ nm}$ and $Em_{595\ nm}$ for Mg-proto and $Ex_{400\ nm}$ and $Em_{630\ nm}$ for proto) with comparison to appropriate standard curves. Unless men-

TABLE 1

Kinetic constants of magnesium chelatase substrates Mg^{2+} and ATP

These values were generated from supplemental Fig. 1. The apparent K_m values for ATP and magnesium were determined with free Mg^{2+} referring to magnesium not forming a complex with ATP. The concentration of free magnesium (Mg^{2+}) was determined with WebMaxClite Version 1.15 software at an ionic strength of 0.05 and 30 °C. Both data sets were fitted to the Michaelis-Menten equation.

Substrate	Apparent V_{max}	Apparent K_m
	nmol Mg-proto/min/nmol BchD	*mM*
Free Mg^{2+}	5.1 ± 0.1	1.3 ± 0.1
ATP	4.5 ± 0.1	0.091 ± 0.009

tioned otherwise, all magnesium chelatase assays were performed using the continuous assay and Mg-proto formation.

ATPase Malachite Green Assays—Assays containing BchI·BchD involved a 1:1 ratio of the two subunits and were refolded on ice as described for magnesium chelatase assays except that 448 nM BchI and BchD with 10 mM DTT were used. Following refolding, BchI·BchD was desalted at 30 °C using NAP-10 or PD-10 columns (GE Healthcare) to remove hydrolyzed ATP and eluted with freshly prepared buffer containing 50 mM Tricine-NaOH (pH 8.0), 15 mM $MgCl_2$, 10 mM DTT, and 2 mM ATP. Assays were performed by addition of 180 μl of desalted BchI·BchD to 180 μl of BchH-proto prepared in 50 mM Tricine-NaOH (pH 8.0), 40 mM glycerol, 15 mM $MgCl_2$, and 1 mM DTT and stopped at five different time points as indicated in the figure legends. The BchH:proto ratio in the assays was 1.26:1. Assays were stopped by addition of a 300-μl sample to 24 μl of 21% (v/v) perchloric acid (ice-cold) and centrifuged at 18,000 × *g* for 7 min at 4 °C. To 100 μl of the supernatant was added 25 μl of freshly prepared malachite green (oxalate) reagent prepared as described previously (37, 38), followed by incubation for 5 min with shaking (1200 rpm) at 20 °C, and the absorbance was read at 620 nm. A standard curve with variable concentrations of Na_2HPO_4 was performed at the same time.

For determining the kinetic parameters, either the Michaelis-Menten equation ($v = V_{max}*[S]/(K_m + [S])$) or the Hill equation ($v = V_{max}*([S]^n)/(k + [S]^n)$) was used for nonlinear regression analysis in GraphPad Prism Version 5.01 for Windows (GraphPad Software, San Diego, CA).

RESULTS

Kinetic Properties of Magnesium Chelatase Substrates Mg^{2+} and ATP—Magnesium is required as a cofactor for the magnesium chelatase assay, and an excess was used in all assays performed. The fits of either variable free magnesium (Mg^{2+}) with fixed ATP or variable ATP with fixed Mg^{2+} were hyperbolic with the apparent K_m for Mg^{2+} being 14-fold higher than that for ATP (Table 1). The amounts of BchI, BchD, and BchH subunits used in these assays were close to optimal (see later experiments).

Proto in the Assay—Two separate BchH-proto preparations were used with different amounts of proto bound. The BchH subunit binds proto maximally in a 1:1 molar ratio (16), and the first BchH used contained a 1.26:1 BchH:proto ratio and is termed near-optimal BchH, whereas the second had a 3.26:1 BchH:proto ratio and is termed proto-depleted BchH. Initial rates were ~1.47 and 0.78 nmol of Mg-proto/min/nmol of BchD for near-optimal and proto-depleted BchH, respectively, and there was some inhibition as the proto was titrated in both cases (Fig. 1*A*). However, despite this slight inhibition, the addi-

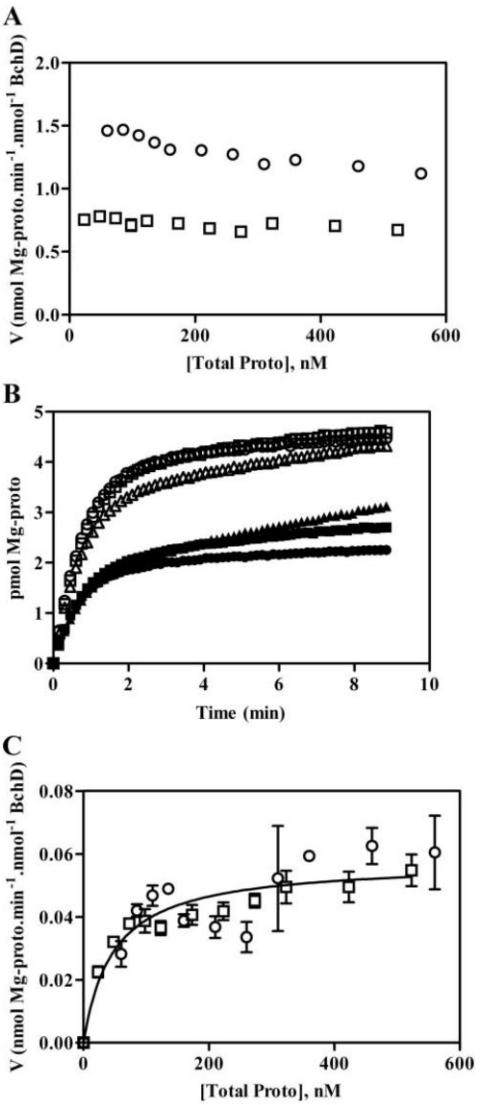

FIGURE 1. **Effect of exogenous proto on magnesium chelatase activity.** Assays were performed with two different BchH stocks, near-optimal (1.26:1) and proto-depleted (3.26:1) BchH-proto. The total proto refers to proto bound to the BchH subunit together with exogenous proto added. Total proto concentrations of 60 and 23 nM refer to proto bound to near-optimal and proto-depleted BchH, respectively, with no exogenous proto added. Assays were performed using 31.6 nM BchI, 15.8 nM BchD, and 75.6 nM BchH. *A*, initial rates with errors given as ±S.D. ○, 1.26:1 BchH:proto stock; □, 3.26:1 BchH:proto stock. *B*, time course following product formation with only three total proto concentrations for each BchH stock shown for clarity: 1.26:1 BchH:proto, 60 nM (○), 110 nM (□), and 560 nM (△); and 3.26:1 BchH:proto, 23 nM (●), 110 nM (■), and 510 nM (▲). *C*, secondary rates determined from 3 to 4.95 min (*B*). *Error bars* indicate the means ± S.D. ○, 1.26:1 BchH:proto stock; □, 3.26:1 BchH:proto stock.

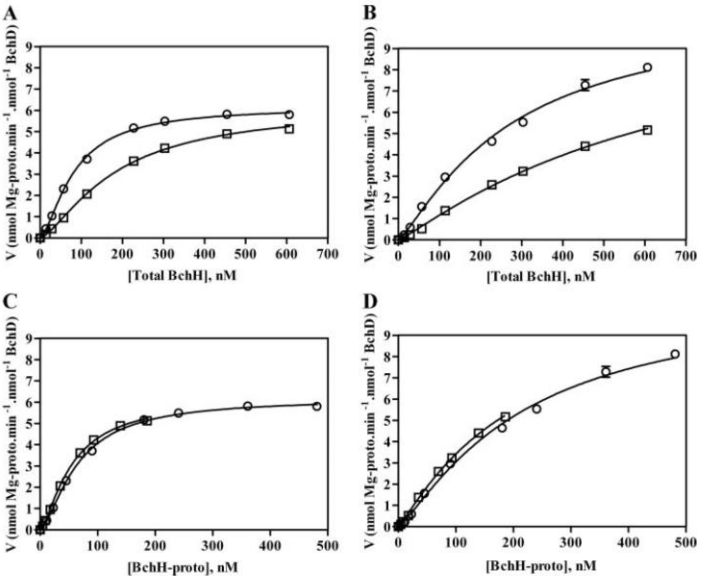

FIGURE 2. **Kinetic analysis of near-optimal and proto-depleted BchH-proto.** ○, near-optimal 1.26:1 BchH:proto stock; □, proto-depleted 3.26:1 BchH:proto stock. Assays were performed using 526 nM BchI with errors given as ±S.D. Shared values were used to determine the apparent V_{max} values for the continuous assays and similarly for the stopped assays. *A*, the continuous assay used 14.2–606 nM BchH, with total BchH referring to the BchH subunit both with and without proto bound. *B*, the stopped assay was performed with total BchH at the same BchH concentrations as indicated above. *C*, the continuous assay was reanalyzed based on the concentration of BchH-proto in the BchH used in the assay. *D*, the stopped assay was reanalyzed referring only to the BchH-proto in the BchH sample.

tional proto was able to participate in the magnesium chelation, as a secondary rate was observed (Fig. 1*B*). This secondary rate, from 3 to 4.95 min, was used to determine a pseudo-K_m and apparent V_{max} for proto (Fig. 1*C*) with both near-optimal and proto-depleted BchH. Both data sets were the same ($p < 0.05$) with a pseudo-K_m for proto of 47 ± 9 nM and an apparent V_{max} of 0.057 ± 0.002 nmol of Mg-proto/min/nmol of BchD. As this apparent V_{max} is the same for both BchH samples but is 14–26-fold lower than the initial rates, the rate-limiting step for the reaction appears to be proto binding to regenerate a functional BchH-proto substrate for the reaction.

BchH as a Substrate—Subsequent experiments utilized BchH-proto as the sole porphyrin substrate without the addition of exogenous proto, and its fate was tested in the magnesium chelatase reaction. Near-optimal and proto-depleted BchH were tested with variable concentrations, and data were analyzed by considering total BchH (BchH containing bound proto as well as BchH with no proto bound). The *v versus* S curves for both BchH types were sigmoidal in both continuous assays (Hill coefficient of 1.4–1.5) (Fig. 2*A*) and stopped assays (Hill coefficient of 1.1–1.2) (Fig. 2*B*), indicating cooperativity, which is discussed further below. When taking into account total BchH, there was a higher apparent $S_{0.5}$ for proto-depleted BchH compared with near-optimal BchH (181 ± 18 and 82 ± 9 nM, respectively), as shown in Fig. 2*A* for the continuous assay. A similar trend was seen using the stopped assay with apparent $S_{0.5}$ values of 656 ± 60 and 276 ± 35 nM for the proto-depleted and near-optimal BchH subunits, respectively (Fig. 2*B*). The difference in apparent $S_{0.5}$ between proto-depleted and near-optimal BchH suggested that the BchH subunit with no proto bound was not participating in the reaction. To test this, it was assumed that only BchH with proto bound (BchH-proto) was contributing to the reaction, and the data were reanalyzed based on the proto bound to BchH (Fig. 2, *C* and *D*). This reanalysis showed that only BchH with proto bound was participating in the reaction and that BchH without proto bound did not interfere with the reaction as shown by the identical sigmoidal curves (Fig. 2*C*). This was also true of the reanalysis of the stopped assays (Fig. 2, compare *B* and *D*). Therefore, BchH without proto bound did not participate and did not apparently adversely affect the magnesium chelation reaction. The remaining experiments considered only BchH-proto as a substrate when determining kinetic constants for the magnesium insertion reaction, and those experiments were performed with near-optimal BchH.

The presence of the reacted BchH subunit (BchH-Mg-proto) was then tested for its effect upon a secondary addition of fresh unreacted BchH-proto. As shown in Fig. 3*A*, the initial magnesium chelatase reaction using 6.1 pmol of BchH-proto was allowed to continue to stationary phase before secondary additions of 3.1, 6.1, or 12.3 pmol of BchH-proto. The initial rates of chelation were 0.52–0.63 nmol of Mg-proto/min/nmol of BchD (Fig. 3*B*, *white bars*). A secondary addition of 6.1 pmol of BchH-proto gave essentially the same velocity as the initial rate (0.55 ± 0.06 nmol of Mg-proto/min/nmol of BchD) as shown in Fig. 3*B* (*6.1 black bar*). Addition of either 12.3 or 3.1 pmol of BchH-proto resulted in the expected higher and lower rates, respectively, compared with the initial rate. The porphyrins extracted following secondary additions also showed an expected increase in Mg-proto levels (Fig. 3*C*). These results show there is no inhibition by BchH-Mg-proto in the magnesium chelation reaction, suggesting that BchH-Mg-proto does not compete with BchH-proto in binding to the BchI·BchD complex.

Assembly of the BchI·BchD Complex—The assembly of the BchI·BchD complex was investigated by varying the concentrations of the BchI and BchD subunits in the magnesium chelatase assay. This is shown in Fig. 4*A* with a variety of curves at different BchD concentrations fit to the Michaelis-Menten equation to generate apparent V_{max} values. A linear relationship was found as the BchD concentration was increased up to 31.7 nM (Fig. 4*B*), therefore, BchD was treated as the "enzyme"

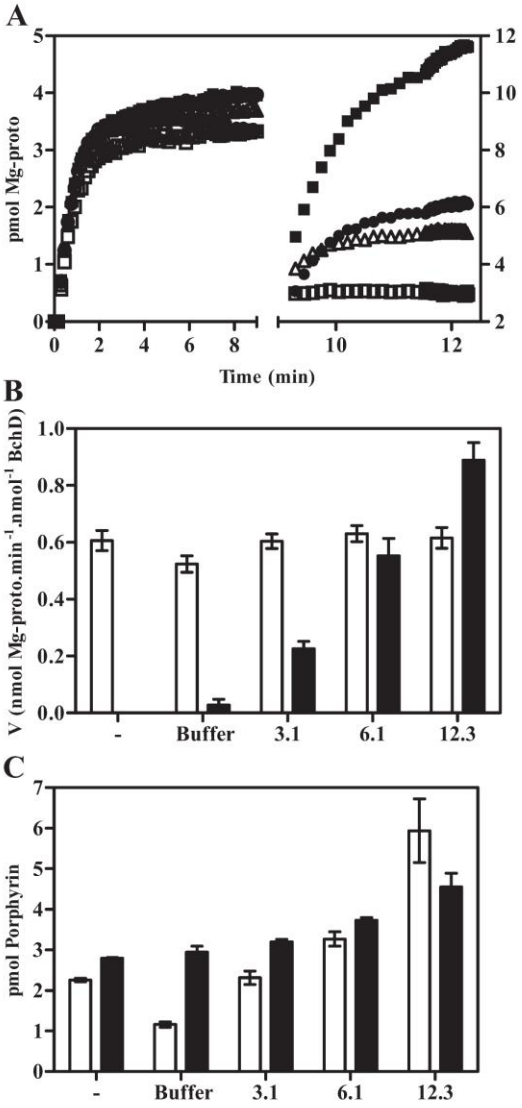

FIGURE 3. **Effect of secondary addition of BchH-proto on rates of magnesium insertion into proto.** All magnesium chelatase initial assays contained 63.2 nM BchI and 30.6 nM BchH-proto (6.1 pmol). Secondary additions (5 μl) involved either assay buffer (as indicated under "Experimental Procedures") or BchH-proto with half (3.1 pmol), equal (6.1 pmol), or double (12.3 pmol) the amount of BchH-proto used in the initial assay. Velocities are given as *V* (nmol of Mg-proto/min/nmol of BchD) ± S.D. *A*, time course monitoring of Mg-proto made (pmol over time). *Left*, initial assay; *right*, secondary additions at 9 min. ○, no secondary addition; □, assay buffer; △, 3.1 pmol of BchH-proto; ■, 6.1 pmol of BchH-proto; ■, 12.3 pmol of BchH-proto. *B*, comparison of initial rates with no secondary addition (−) and secondary additions of the BchH-proto subunit. *Error bars* represent the means ± S.D. *White bars*, initial velocities of the initial assay; *black bars*, secondary addition of either BchH-proto or assay buffer. Secondary additions of BchH-proto or assay buffer were stopped using acetone/ammonia at 12.3 min. *C*, extracted porphyrin amounts using acetone/ammonia after 9 min (−) or after the secondary assay buffer or BchH-proto additions at 12.3 min. *White bars*, Mg-proto levels extracted; *black bars*, proto levels extracted.

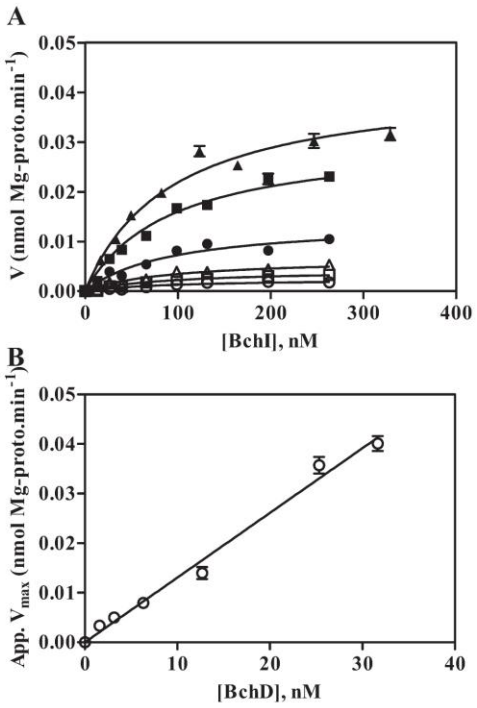

FIGURE 4. **Kinetic properties of the BchD subunit in magnesium chelatase assays.** Variable concentrations of BchI (13.2–329 nM) were used at fixed BchD concentrations (1.58 nM (○), 3.16 nM (□), 6.33 nM (△), 12.7 nM (●), 25.3 nM (■), and 31.7 nM (▲)), and the BchI:BchD ratios were at least 0.5:1. *A*, the Michaelis-Menten equation was fitted to the data to generate apparent V_{max} values for the given BchD concentrations. *Error bars* represent the means ± S.D. *B*, apparent V_{max} values generated in *A* are plotted against the fixed BchD concentrations, and linear regression was applied and fitted through zero.

in all analyses, and activities are given as per nmol of BchD subunit in all other experiments. Two substrate kinetic analyses assuming BchI and BchH-proto as the two substrates were conducted at fixed BchD concentrations (Fig. 5). A sigmoidal relationship was clearly observed with BchH as the substrate (Fig. 5*A*), indicating cooperativity at all BchI concentrations. The secondary plot of the apparent V_{max} against BchI concentration (Fig. 5*B*) was clearly hyperbolic with a K_m for BchI of 20.2 ± 3.2 nM and V_{max} of 5.1 ± 0.3 nmol of Mg-proto/min/nmol of BchD.

ATPase Activity of the BchI·BchD Complex—The BchI subunit contains low intrinsic ATPase activity. The ATPase activity of BchI·BchD was 1.66-fold higher compared with that of BchI, and both exhibited a linear response over the concentrations tested (Fig. 6). Negligible ATPase activity was detected from BchH-proto (supplemental Fig. 2) (39). Addition of BchH-proto to produce a complete magnesium chelatase (BchI·BchD·BchH-proto) complex caused an ~33-fold increase in the rate of ATPase activity of the BchI·BchD complex (Table

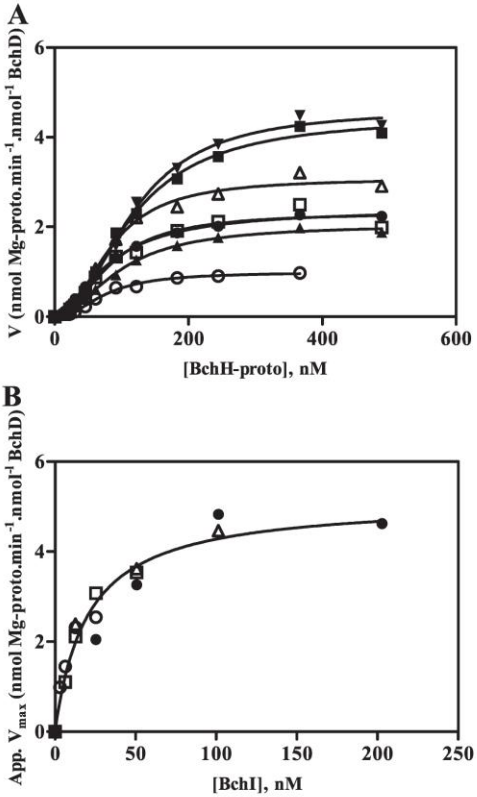

FIGURE 5. **Kinetic properties of the BchI subunit in magnesium chelatase assays.** Variable concentrations of BchH-proto (11.5–489 nM) were used at fixed combinations of BchI (3.16–202 nM) and BchD (3.16–25.3 nM). Glycerol concentrations were from 15.5 to 21 mM. *A*, the Hill equation was fitted to the data to generate apparent V_{max} values for the given BchI concentrations. *Error bars* represent the means ± S.D. Only 7 of 16 of the fixed data sets are shown for clarity: 3.16 nM BchD and 3.16 nM BchI (○), 3.16 nM BchD and 12.6 nM BchI (□), 6.3 nM BchD and 25.3 nM BchI (△), 12.6 nM BchD and 12.6 nM BchI (●), 12.6 nM BchD and 101 nM BchI (■), 25.3 nM BchD and 25.3 nM BchI (▲), and 25.3 nM BchD and 202 nM BchI (▼). *B*, apparent V_{max} values generated in *A* are plotted against the fixed concentrations of BchI with the Michaelis-Menten equation fitted to the data. The four variable BchD concentrations are plotted on the same graph: 3.16 nM (○), 6.3 nM (□), 12.6 nM (△), and 25.3 nM (●).

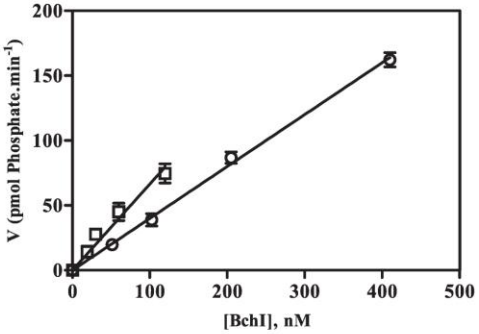

FIGURE 6. **ATPase activity of the BchI subunit and BchI·BchD complex.** ○, BchI assay; □, BchI·BchD assay. Assays were performed for 5, 10, 15, 20, and 30 min.

TABLE 2

Comparison of the ATPase and magnesium chelatase activities of the BchI·BchD·BchH-proto complex

All values were determined from supplemental Fig. 2 (*A–C*) with the same final concentrations for each assay with limiting BchI to allow comparison of ATPase and magnesium chelatase activities. Two different types of magnesium chelatase assays (continuous and stopped) were used with variable BchH-proto concentrations (15–481 nM). Hill equations were applied to each experiment, giving apparent V_{max} values (nmol/min/nmol of BchD or BchI), with the resulting apparent $S_{0.5}$ values referring to BchH-proto.

Substrate	Apparent V_{max}	Apparent $S_{0.5}$	Hill coefficient
		nM	
ATPase	128 ± 6	119 ± 48	2.27 ± 0.27
Magnesium chelatase (continuous)	2.71 ± 0.05	61 ± 12	2.00 ± 0.11
Magnesium chelatase (stopped)	3.10 ± 0.10	118 ± 45	1.29 ± 0.15

TABLE 3

Summary of kinetic constants for the magnesium chelatase protein substrates BchI and BchH-proto

These values were generated from Figs. 5*B* and 7*B*, with V_{max} given as nmol of Mg-proto/min/nmol of BchD and K_{cat} given as min^{-1}.

Substrate	V_{max} or K_{cat}	K_m	Hill coefficient	$S_{0.5}$	$K_{cat}/(K_m$ or $S_{0.5})$
		nM		nM	$min^{-1}\ M^{-1} \times 10^6$
BchI	5.1 ± 0.3	20.2 ± 3.2			252
BchH-proto	5.4 ± 0.1		1.85 ± 0.06	132 ± 20	41

2). The ATPase activity of BchI·BchD·BchH-proto was expressed per nmol of BchI subunit because this is the only magnesium chelatase subunit with ATPase activity; however, a 1:1 BchI:BchD ratio was used in these experiments, and hence, ATPase activity is directly comparable with magnesium chelatase activity. The apparent V_{max} of ATPase activity was 41- and 47-fold higher compared with the corresponding apparent V_{max} for magnesium chelatase activity using the stopped and continuous assays, respectively. However, the rate of magnesium insertion was only linear for ~30 s, whereas the rate of ATP hydrolysis was linear for >30 min and continued after magnesium insertion had ceased (supplemental Fig. 2, *D* and *E*). The differences in apparent V_{max} in Table 2 compared with Table 3 are due to suboptimal BchI concentrations used to generate Table 2 data to allow for ATPase measurements with a minimum background of ATPase activity from the BchI subunit.

Cooperativity of the BchH-Proto Subunit—Two substrate kinetic analyses with BchI and BchH-proto treated as the substrates were performed (Fig. 7*A*). A sigmoidal plot was obtained when the apparent V_{max} values for BchI were plotted against BchH-proto concentrations (Fig. 7*B*) and gave a Hill coefficient of 1.85 and an $S_{0.5}$ of 132 ± 20 nM. This sigmoidal curve was obtained when measuring both magnesium chelation activity and ATPase activity and resulted in similar Hill coefficients: 2.0 and 2.3 (Table 2). However, the apparent $S_{0.5}$ value was 2-fold higher for the ATPase activity compared with the magnesium chelatase activity in a continuous assay (Table 2). The apparent $S_{0.5}$ and Hill constants obtained with stopped assays were significantly different from those obtained with continuous assays, with stopped assays approaching hyperbolic curves. This was also observed in previous experiments (Fig. 2). The reason for

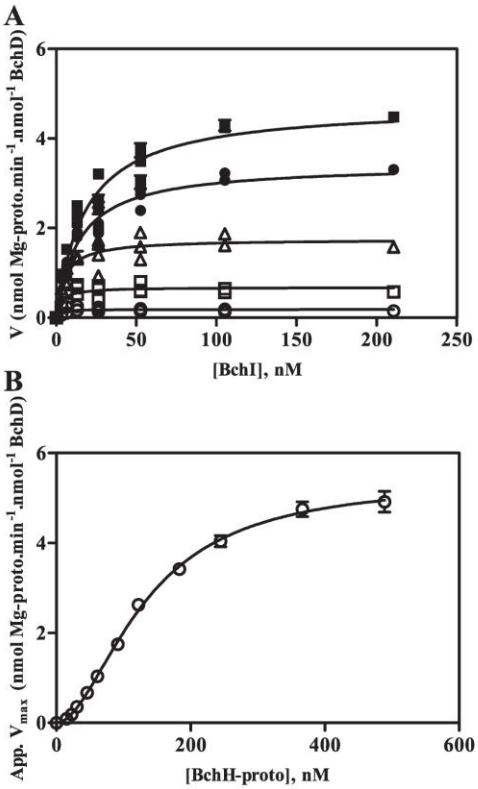

FIGURE 7. **Kinetic properties of the BchH-proto subunit in magnesium chelatase assays.** Variable concentrations of BchI (13.2–263 nM) and BchD (1.58–31.7 nM) were used at fixed concentrations of BchH-proto (15, 23, 31, 46, 61, 92, 122, 183, 244, 367, and 489 nM). Glycerol concentrations were from 15.5 to 21 mM. *A*, the Michaelis-Menten equation was fitted to the data to generate apparent V_{max} values for the given BchH-proto concentrations. *Error bars* represent the means ± S.D. Only 5 of 12 fixed BchH-proto concentrations are shown for clarity: 23 nM (○), 46 nM (□), 92 nM (△), 183 nM (●), and 367 nM (■). *B*, the apparent V_{max} values generated in *B* are plotted against the fixed concentrations of BchH-proto with the Hill equation fitted to the data.

the differences between the stopped and continuous assays appears to be due to loss of magnesium from Mg-proto when stopping the assay. This loss of magnesium from Mg-proto was reduced or absent when the assay was stopped after magnesium chelation had apparently ceased, suggesting that the chelation reaction proceeds through an intermediate labile form of Mg-proto.

In summary, the kinetic properties of the BchI and BchH-proto protein subunits for the BchD enzyme are quite different (Table 3). The BchI subunit has a K_m of 20 nM and does not display cooperativity, whereas the BchH-proto subunit has an $S_{0.5}$ of 132 nM and shows cooperativity. Thus, the BchI subunit forms a tight association with BchD to form a BchI·BchD complex, with BchH forming a transient substrate-like association with the BchI·BchD complex. This is consistent with previous data from *Synechocystis,* for which the K_m values for the BchI and BchH subunits were 85–107 and 200–260 nM, respectively

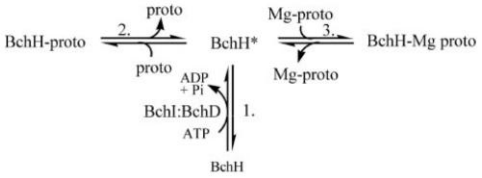

SCHEME 1

(17). Therefore, rates of chelation are most sensitive to BchH concentration as implied previously (40). Also, the K_{cat} for magnesium chelation was 5.1–5.4 min^{-1} and was ~6-fold higher compared with that using purified *Synechocystis* enzyme and deuteroporphyrin as a substrate (19).

DISCUSSION

The BchH subunit of magnesium chelatase from *R. capsulatus* bound the porphyrin substrate, proto, very tightly such that it was difficult to remove without loss of enzyme activity. This differs from the *Synechocystis* homolog ChlH, whereupon the proto is lost during anion-exchange chromatography (17). Therefore, in our experiments, the BchH-proto subunit effectively acted as the porphyrin substrate for the magnesium chelatase reaction, and activity could be measured without addition of proto. In our experiments, proto remained tightly bound to the BchH subunit even after extensive washing with detergent during purification. Therefore, we could not determine a real K_m value for proto using normal steady-state kinetics of the initial rate. However, we found that addition of exogenous proto resulted in a continued increase in Mg-proto made compared with no additional proto. This allowed us to calculate a pseudo-K_m for proto using the continued increase in rates with addition of variable proto (Fig. 1*C*) at a fixed BchH concentration. The effect of proto addition was tested on two BchH preparations, near-optimal and proto-depleted BchH. The pseudo-K_m for proto of 47 nM with either near-optimal or proto-depleted BchH is significantly lower than previous results obtained with *R. sphaeroides* (150 nM) (15) and *Synechocystis* and *R. capsulatus* (1250 and 1230 nM, respectively) (14, 17). This pseudo-K_m for proto approaches the K_m values reported for chloroplast preparations from pea leaves and cucumber: 13.5 and 25 nM, respectively (12, 13).

These data suggest a role for BchI·BchD in facilitating binding of porphyrin as shown in Scheme 1 (*step 1*). Mg-proto usually remains bound to the BchH subunit following chelation (23), but we observed an additional amount of Mg-proto made with exogenous proto. This suggests that Mg-proto normally stays bound to BchH unless exogenous proto is present, with which it can be exchanged. Although proto does appear to bind to proto-depleted BchH when mixed and preincubated (14), it is not in a state that can immediately participate in magnesium chelation (see Fig. 1 and previous results). This implies that BchH* shown in Scheme 1 is a transient porphyrin-binding intermediate form of BchH. The binding of proto to BchH* appears to be the rate-limiting step in magnesium chelation because the secondary rate of catalysis has a 14- and 26-fold lower rate than the initial rates of the proto-depleted and near-optimal BchH samples tested (Fig. 1, *A* and *C*). This loading of

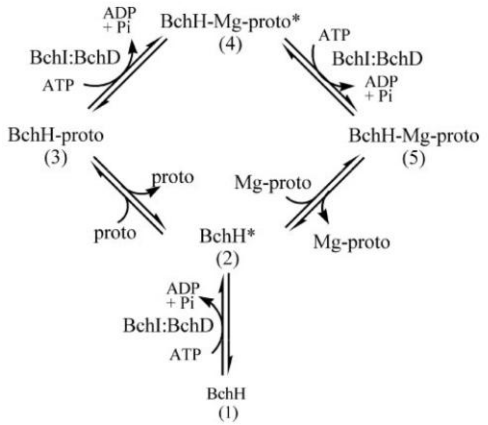

SCHEME 2

proto onto BchH may be explained by extensive conformational changes of the BchH subunit, possibly by the BchI·BchD complex. The Mg-proto released does not have a large inhibitory impact on magnesium chelation, with only 16% inhibition at 71 nM Mg-proto. The rate of binding of proto to BchH may be higher *in vivo* if it is facilitated by a bacterial equivalent to the plant protein Gun4, which acts like a proto chaperone (4–6), and a candidate for this has been suggested to be BchJ (7, 8).

The question arises as to whether *steps 2* and *3* in Scheme 1 require BchI·BchD and/or ATP hydrolysis. The lack of inhibition by BchH-Mg-proto suggests that BchH-Mg-proto does not bind to BchI·BchD or does not compete very well with BchH-proto for binding to BchI·BchD. The latter is one possibility because proto-depleted BchH did not compete with BchH-proto for binding to BchI·BchD as shown by the data in Fig. 2. This suggests that the BchH subunit with Mg-proto dissociates from the BchI·BchD complex and allows binding of unreacted BchH-proto substrate. Also BchH-Mg-proto does not inhibit further binding of the BchH-proto substrate to BchI·BchD.

The stopped assay gave lower initial rates and a different kinetic profile compared with the continuous assay (Fig. 3, *A* and *C*). This appears to be due to loss of magnesium from the proto during extraction rather than to any fluorescent artifact. This suggests that there is an intermediate bound form of Mg-proto that is unstable when the proteins are denatured to extract the porphyrin.

The BchI subunit and BchI·BchD complex show relatively low ATPase activity that is stimulated by 33-fold upon addition of the BchH subunit to the latter (Table 2). A 16–20-fold increase in ATPase activity was observed with *Synechocystis* (28). The binding of the BchH subunit to BchI·BchD therefore triggers faster ATP hydrolysis. The kinetics of the ATPase activity stimulation by BchH has an ~41–47-fold greater V_{max} compared with magnesium chelatase activity. This is ~3-fold higher than the value obtained in a previous report using *Synechocystis* that showed a 15:1 ratio of ATP hydrolyzed for every magnesium inserted into deuteroporphyrin, the water-soluble analog of proto (19). The purpose of the additional hydrolysis of ATP is unclear; however, considering that there is strong kinetic data (shown here) and structural evidence (23) for multiple forms of BchH, it seems likely that ATP hydrolysis by BchI·BchD functions to modify the conformation of BchH through a sequential series of conformational changes. The model for catalysis shown in Scheme 2 has a minimum of five conformational forms for BchH that are consistent with the data presented here. These five forms in a catalytic cycle would be 1) BchH, a form that does not specifically bind proto; 2) BchH*, a form capable of binding proto; 3) BchH-proto; 4) BchH-Mg-proto*, a labile intermediate form of BchH; and 5) BchH-Mg-proto. The BchH with no proto bound (form 1) cannot bind proto readily and needs to change conformations by interacting with the BchI·BchD complex, which drives this process by hydrolyzing ATP and gives BchH* (form 2). The BchH* can now bind proto to form BchH-proto (form 3), the substrate for magnesium chelation by BchI·BchD. Chelation produces an unstable BchH-Mg-proto* intermediate (form 4), which can lose magnesium in basic conditions with acetone. This is then converted to a stable BchH-Mg-proto product (form 5). In the presence of exogenous proto and BchI·BchD, Mg-proto is released from BchH, and the cycle can continue from form 2. It should be qualified that the necessity for ATP hydrolysis at each transition is speculative.

Interestingly, the ATPase activity of BchI·BchD·BchH-proto continues at a similar rate after the magnesium chelation has stopped, suggesting that the trigger for ATP hydrolysis is simply binding of BchH in any conformation. From a regulatory point of view, a second molecule/protein may be required *in vivo* to halt the BchI·BchD ATPase activity cycle once magnesium has been inserted, for example, by binding to BchH and stopping its interaction with BchI·BchD. One possibility for this is BchM/ChlM, the next enzyme in the biosynthetic pathway, because interactions between BchM/ChlM and BchH have been reported (41–44).

Assembly of the BchI·BchD Complex—A previous report suggested that the BchD subunit acts as a platform for binding of the BchI and BchH subunits to form the complete functional magnesium chelatase complex (21). This type of arrangement suggests that the BchD subunit is acting as an enzyme with the BchI and BchH subunits behaving as substrates, and this was also seen in a previous study with *Synechocystis* (17). In our study, the behavior of BchD was tested by keeping it at a fixed concentration while varying the BchI concentration. A linear response was obtained when plotting apparent V_{max} *versus* BchD concentration, suggesting that the BchD subunit in the 1.58–31.7 nM range can be treated as the enzyme in the analyses. The K_m of the BchI subunit was found to be 20 ± 3.2 nM, which means that only 50% of the BchD forms functional BchI·BchD complexes at this BchI concentration (Fig. 5*B*). Approximately 100–200 nM BchI is required to form a fully functional BchI·BchD complex, and BchI needs to be in excess over BchD. These results are consistent with previous studies showing that an excess of BchI subunit is required for optimal magnesium chelatase activity (14, 15, 17) and highlight the dynamic nature of the BchI·BchD complex *in vitro*.

Cooperativity and Regulation of Pigment Synthesis—Magnesium chelatase commits proto to chlorophyll/bacteriochloro-

phyll synthesis, and as such, it has been regarded as a regulated step. In the chlorophyll-synthesizing pea and *Synechocystis*, cooperativity is observed with Mg^{2+} (12, 17, 19), suggesting that magnesium concentrations play a role in this regulation. In addition, cooperativity has also been observed for ATP with the pea enzyme (12). In contrast, bacteriochlorophyll-synthesizing *R. capsulatus* does not exhibit cooperativity with either of these substrates (Table 1 and supplemental Fig. 1) (15). Thus, it appears the cyanobacterial and plant enzymes are regulated by magnesium concentration.

The cooperativity observed for BchH-proto in both the ATPase and continuous magnesium chelatase assays (Hill coefficient of 1.85–2.3) (Tables 2 and 3) indicates that more than one BchH-proto subunit is involved in binding to the BchI·BchD complex. Based on the EM studies (24, 33) in which BchI and BchI·BchD are hexameric and form a dimer of trimers or a trimer of dimers, a Hill coefficient of 2 suggests that either two or three BchH-proto subunits bind per BchI·BchD complex. Thus, the concentration of the BchH subunit is an important factor in regulation of the *R. capsulatus* enzyme, and this is consistent with the regulation of BchH stability *in vivo* by light and oxygen levels (40).

Conclusion—Our results show that the BchI and BchH-proto subunits can be treated as protein substrates for the BchD subunit in a kinetic analysis. The BchH-proto subunit shows cooperativity with both magnesium chelatase and ATPase activities with a Hill coefficient of ~2. This, together with EM structural studies (24, 33), indicates that either two or three BchH-proto subunits bind per BchI·BchD complex. It was found that the ATPase activity of BchI·BchD is stimulated by BchH-proto, with the maximum rate of ATP hydrolysis being ~40-fold greater than the maximum rate of magnesium chelation, similar to a previous report with *Synechocystis* (19). ATP hydrolysis continues despite magnesium chelation ceasing, which suggests that binding of BchH triggers ATP hydrolysis in BchI·BchD. The results indicate that BchH exists in at least five conformational forms both with and without proto or Mg-proto bound and that BchI·BchD hydrolyzes ATP to induce a series of conformational changes in BchH to facilitate magnesium insertion, Mg-proto release, and proto binding. Proto binding to BchH appears to be the rate-limiting step in the proposed magnesium chelatase reaction model.

REFERENCES

1. Hanson, P. I., and Whiteheart, S. W. (2005) *Nat. Rev. Mol. Cell Biol.* **6,** 519–529
2. Vale, R. D. (2000) *J. Cell Biol.* **150,** 13F–20F
3. Willows, R. D., and Hansson, M. (2003) in *The Porphyrin Handbook* (Kadish, K. M., Smith, K. M., and Guilard, R., eds) pp. 1–47, Academic Press, Sydney, Australia
4. Davison, P. A., Schubert, H. L., Reid, J. D., Iorg, C. D., Heroux, A., Hill, C. P., and Hunter, C. N. (2005) *Biochemistry* **44,** 7603–7612
5. Larkin, R. M., Alonso, J. M., Ecker, J. R., and Chory, J. (2003) *Science* **299,** 902–906
6. Verdecia, M. A., Larkin, R. M., Ferrer, J.-L., Riek, R., Chory, J., and Noel, J. P. (2005) *PLoS Biol.* **3,** e151
7. Chew, A. G. M., and Bryant, D. A. (2007) *Annu. Rev. Microbiol.* **61,** 113–129
8. Chew, A. G. M., and Bryant, D. A. (2007) *J. Biol. Chem.* **282,** 2967–2975
9. Reid, J. D., and Hunter, C. N. (2002) *Biochem. Soc. Trans.* **30,** 643–645
10. Walker, C. J., and Willows, R. D. (1997) *Biochem. J.* **327,** 321–333
11. Masuda, T. (2008) *Photosynth. Res.* **96,** 121–143
12. Guo, R., Luo, M., and Weinstein, J. D. (1998) *Plant Physiol.* **116,** 605–615
13. Richter, M. L., and Rienits, K. G. (1982) *Biochim. Biophys. Acta* **717,** 255–264
14. Willows, R. D., and Beale, S. I. (1998) *J. Biol. Chem.* **273,** 34206–34213
15. Gibson, L. C. D., Jensen, P. E., and Hunter, C. N. (1999) *Biochem. J.* **337,** 243–251
16. Willows, R. D., Gibson, L. C. D., Kanangara, C. G., Hunter, C. N., and von Wettstein, D. (1996) *Eur. J. Biochem.* **235,** 438–443
17. Jensen, P. E., Gibson, L. C. D., and Hunter, C. N. (1998) *Biochem. J.* **334,** 335–344
18. Karger, G. A., Reid, J. D., and Hunter, C. N. (2001) *Biochemistry* **40,** 9291–9299
19. Reid, J. D., and Hunter, C. N. (2004) *J. Biol. Chem.* **279,** 26893–26899
20. Viney, J., Davison, P. A., Hunter, C. N., and Reid, J. D. (2007) *Biochemistry* **46,** 12788–12794
21. Axelsson, E., Lundqvist, J., Sawicki, A., Nilsson, S., Schroder, I., Al-Karadaghi, S., Willows, R. D., and Hansson, M. (2006) *Plant Cell* **18,** 3606–3616
22. Fodje, M. N., Hansson, A., Hansson, M., Olsen, J. G., Gough, S., Willows, R. D., and Al-Karadaghi, S. (2001) *J. Mol. Biol.* **311,** 111–122
23. Sirijovski, N., Lundqvist, J., Rosenback, M., Elmlund, H., Al-Karadaghi, S., Willows, R. D., and Hansson, M. (2008) *J. Biol. Chem.* **283,** 11652–11660
24. Willows, R. D., Hansson, A., Bircha, D., Al-Karadaghi, S., and Hansson, M. (2004) *J. Struct. Biol.* **146,** 227–233
25. Willows, R. D., Hansson, M., Beale, S. I., Laurberg, M., and Al-Karadaghi, S. (1999) *Acta Crystallogr. Sect. D* **55,** 689–690
26. Reid, J. D., Siebert, C. A., Bullough, P. A., and Hunter, C. N. (2003) *Biochemistry* **22,** 6912–6920
27. Hansson, M., and Kannangara, C. G. (1997) *Proc. Natl. Acad. Sci. U. S. A.* **94,** 13351–13356
28. Jensen, P. E., Gibson, L. C. D., and Hunter, C. N. (1999) *Biochem. J.* **339,** 127–134
29. Petersen, B. L., Kannangara, C. G., and Henningsen, K. W. (1999) *Arch. Microbiol.* **171,** 146–150
30. Gräfe, S., Saluz, H.-P., Grimm, B., and Hänel, F. (1999) *Proc. Natl. Acad. Sci. U. S. A.* **96,** 1941–1946
31. Lake, V., Olsson, U., Willows, R. D., and Hansson, M. (2004) *Eur. J. Biochem.* **271,** 2182–2188
32. Papenbrock, J., Gräfe, S., Kruse, E., Hänel, F., and Grimm, B. (1997) *Plant J.* **12,** 981–990
33. Elmlund, H., Lundqvist, J., Al-Karadaghi, S., Hansson, M., Hebert, H., and Lindahl, M. (2008) *J. Mol. Biol.* **375,** 934–947
34. Bradford, M. M. (1976) *Anal. Biochem.* **72,** 248–254
35. Sawicki, A., and Willows, R. D. (2007) *Biochem. J.* **406,** 469–478
36. Hansson, A., Willows, R. D., Roberts, T. H., and Hansson, M. (2002) *Proc. Natl. Acad. Sci. U. S. A.* **99,** 13944–13949
37. Baykov, A. A., Evtushenko, O. A., and Avaeva, S. M. (1988) *Anal. Biochem.* **171,** 266–270
38. Geladopoulos, T. P., Sotiroudis, T. G., and Evangelopoulos, A. E. (1991) *Anal. Biochem.* **192,** 112–116
39. Sirijovski, N., Olsson, U., Lundqvist, J., Al-Karadaghi, S., Willows, R. D., and Hansson, M. (2006) *Biochem. J.* **400,** 477–484
40. Willows, R. D., Lake, V., Roberts, T. H., and Beale, S. I. (2003) *J. Bacteriol.* **185,** 3249–3258
41. Alawady, A., Reski, R., Yaronskaya, E., and Grimm, B. (2005) *Plant Mol. Biol.* **57,** 679–691
42. Shepherd, M., McLean, S., and Hunter, C. N. (2005) *FEBS J.* **272,** 4532–4539
43. Gorchein, A. (1972) *Biochem. J.* **127,** 97–106
44. Hinchigeri, S. B., Hundle, B., and Richards, W. R. (1997) *FEBS Lett.* **407,** 337–342

3.3 Supplementary data

Supplementary Fig. 1. Kinetic constants of magnesium chelatase substrates; Mg^{2+}, and ATP. Free magnesium (Mg^{2+}) refers to magnesium not complexed with ATP. All assays were performed using 225 nM BchI, 457 nM BchH-proto and data fitted to the Michaelis-Menten equation with error bars stated as ± S.D. *A*. Assays were performed at 1 mM ATP with variable Mg^{2+} concentrations; 0.035, 0.080, 0.35, 0.57, 0.80, 1.0, 2.0, 3.0, 5.0, 7.0, 9.0, 11.5, 14.0, 19.0 mM. *B*. Assays were performed at 15 mM $MgCl_2$ with variable ATP concentrations; 0.025, 0.05, 0.1, 0.2, 0.4, 0.6, 0.8, 1, 2.5, 5 mM.

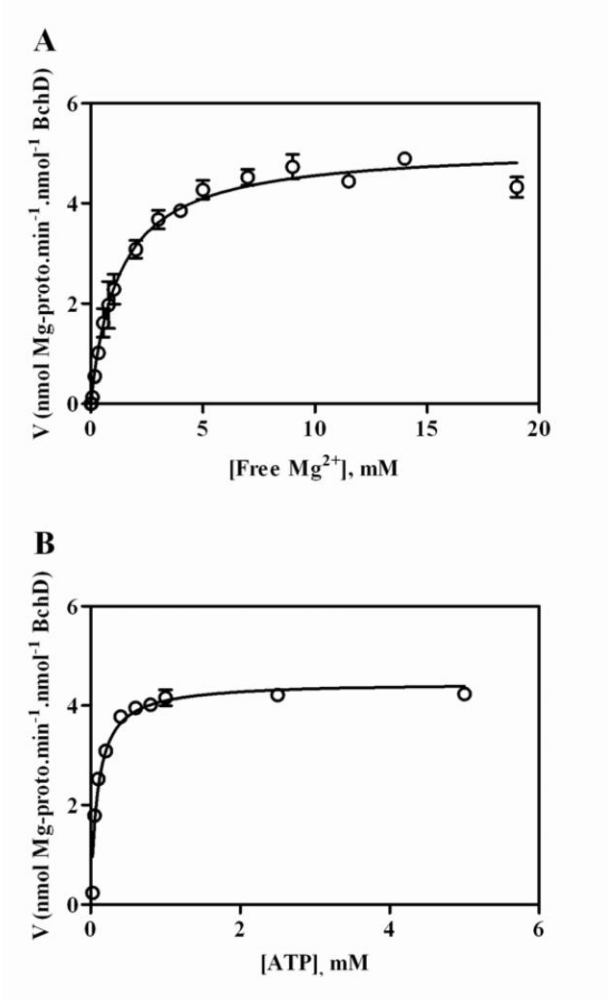

Supplementary Fig. 2. Comparison of ATPase and magnesium chelatase activity of BchI:BchD:BchH-proto. Variable concentrations of BchH-proto were used; 15, 30, 60, 120, 241, 481, 962 nM, with only four concentrations shown for clarity; ○ 30, □ 60, Δ 120, ● 481 nM. Final assay concentrations were 50 mM Tricine-NaOH pH 8.0, 20 mM glycerol, 15 mM $MgCl_2$, 5.5 mM DTT, 1 mM ATP, 26 nM BchI and 26 nM BchD with error bars stated as ± S.D. *A*. ATPase activity of BchI:BchD:BchH-proto, with the BchI:BchD activity deducted from each BchH-proto concentration used. Depending upon the BchH-proto concentration, each assay was performed at five time points in the range, 0.5-60 min. BchH-proto alone at 962 nM exhibited 2.45 % of the activity compared with BchI:BchD:BchH-proto *B*. Magnesium chelatase activity using continuous assay *C*. Magnesium chelatase activity using stopped assay *D*. ATPase time course *E*. Magnesium chelatase time course using stopped assay

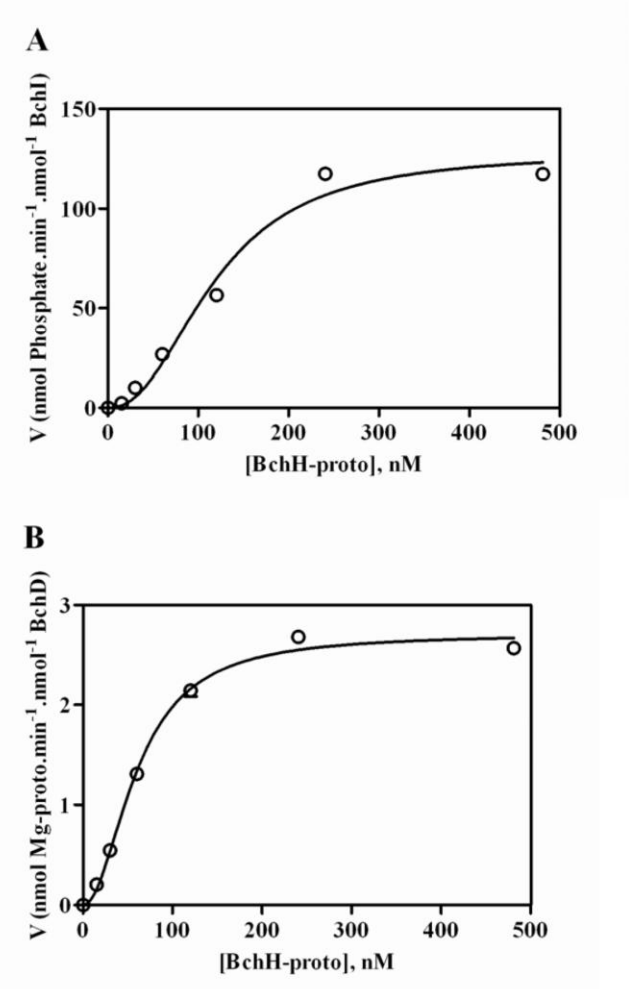

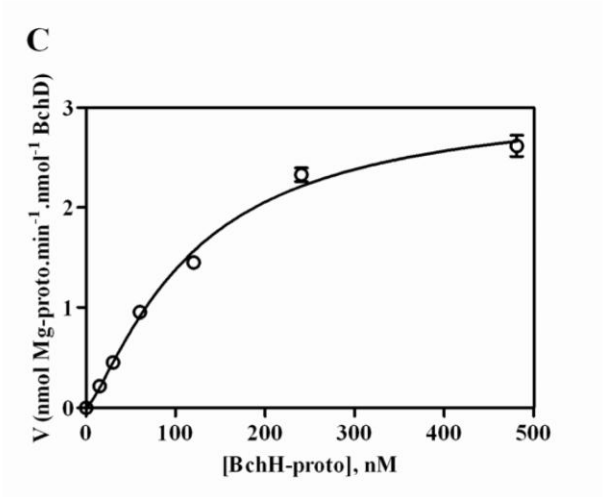
C
V (nmol Mg-proto.min-1.nmol-1 BchD)
0
1
2
3
0
100
200
300
400
500
[BchH-proto], nM

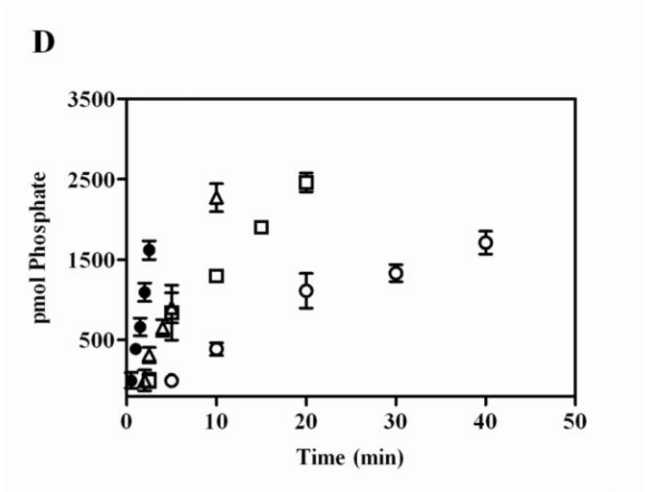
D
pmol Phosphate
500
1500
2500
3500
0
10
20
30
40
50
Time (min)

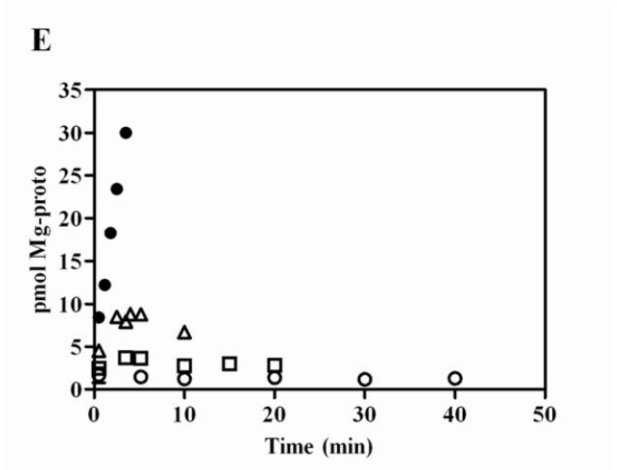
E
pmol Mg-proto
0
5
10
15
20
25
30
35
0
10
20
30
40
50
Time (min)

3.4 Addendum

Kinetic Analyses of the Magnesium Chelatase Provide Insights into the Mechanism, Structure, and Formation of the Complex. Artur Sawicki and Robert D. Willows VOLUME 283 (2008) PAGES 31294-31302

During further analysis of the magnesium chelatase BchI▪BchD complex, it was found that the free magnesium concentration calculated in this study was incorrectly determined. No account was taken for the magnesium content associated with the protein solutions and we apologize for this mistake. After re-analysis, a co-operative effect (Hill constant of 2.15) was found with free magnesium, not the originally stated hyperbolic relationship. This was repeated several times with two separate protein preparations on separate days (four triplicate sets for most of the data and at least two triplicate sets), and the culmination of this data was combined to produce the revised Supplementary Figure 1a. This amended data now agrees with several previous experiments from pea, cucumber, *Synechocystis*, and green sulphur bacterium, *Chlorobaculum tepidum* which indicated the regulatory effect of free magnesium on magnesium chelatase activity (Richter and Reinits, 1982; Guo et al. 1998; Jensen et al. 1998; Reid and Hunter, 2004; Johnson and Schmidt-Dannert, 2008). The updated kinetic results for free magnesium on magnesium chelatase summarized in the revised Table 1 now highlight the sigmoidal nature of the substrate in the purple non-sulphur bacterium *Rba. capsulatus*.

Table 1. Revised kinetic constant of magnesium chelatase substrate; Mg^{2+}.

The revised kinetic constant for free magnesium was determined from Appended Supplementary Fig. 1a with App.V_{max} stated as (nmol Mg-proto.min^{-1}.$nmol^{-1}$ BchD). The apparent $S_{0.5}$ value for free magnesium was newly determined by taking into account the magnesium present in BchI, BchD, and BchH-proto solutions. The new results were fit to the Hill equation, whereas the kinetic properties of ATP substrate remained the same, and could not be fit to the Hill equation.

Substrate	App.V_{max}	App.K_m or $S_{0.5}$ (mM)	Hill constant
Free Mg^{2+}	4.4 ± 0.04	1.3 ± 0.04	2.15 ± 0.1
ATP	4.5 ± 0.1	0.091 ± 0.009	N.D.

Supplementary Fig. 1. Revised kinetic constants of the magnesium chelatase substrate; Mg^{2+}.

A. Free magnesium (Mg^{2+}) was newly determined by taking into account the magnesium content present in BchI, BchD, and BchH-proto solutions with error bars stated as ± S.D. Assays were performed at 1 mM ATP with variable Mg^{2+} concentrations; 0.028, 0.14, 0.29, 0.49, 0.72, 0.95, 1.2, 1.4, 2.4, 3.4, 4.4, 5.4, 7.3, 9.3, 11.8, 14.3, 19.2, 29.1 mM. *B*. Assays were performed at 15 mM $MgCl_2$ with variable ATP concentrations; 0.025, 0.05, 0.1, 0.2, 0.4, 0.6, 0.8, 1, 2.5, 5 mM. This Figure did not change.

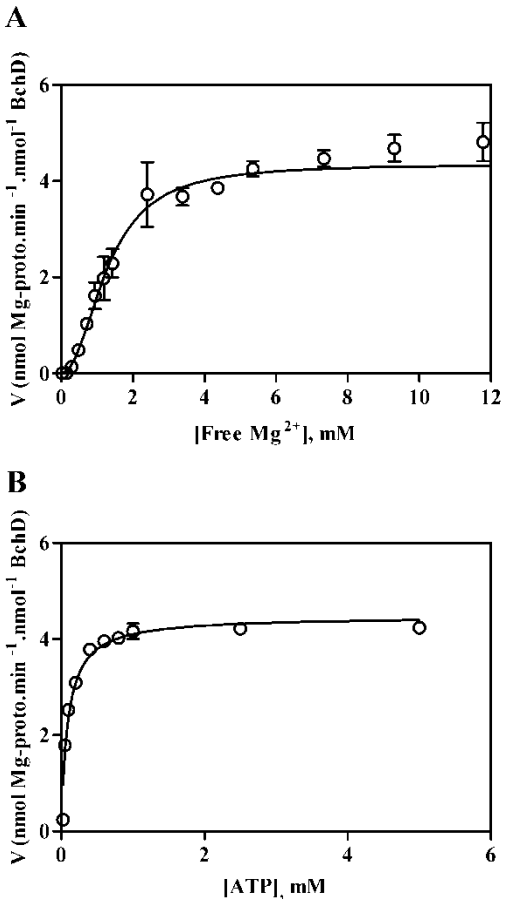

REFERENCES

1. Guo, R., Luo, M., and Weinstein, J. D. (1998) *Plant Physiol*. **116**, 605-615

2. Jensen, P. E., Gibson, L. C. D., and Hunter, C. N. (1998) Biochem. J. **334**, 335-344

3. Johnson, E. T., and Schmidt-Dannert, C. (2008) *J. Biol. Chem*. **283**, 27776-27784

4. Reid, J. D., and Hunter, C. N. (2004), *J. Biol. Chem*. **279**, 26893-26899

5. Richter, M. L. and Reinits, K. G. (1982), *Biochim. Biophys. Acta* **717**, 255-264